

PHASES OF DENSE MATTER IN NEUTRON STARS

Henning Heiselberg

NORDITA, Blegdamsvej 17, DK-2100 Copenhagen Ø, Denmark

Abstract

After a brief history of neutron stars and supernovae recent developments are discussed. Based on modern nucleon-nucleon potentials more reliable equations of state for dense nuclear matter have been constructed. Furthermore, phase transitions such as pion, kaon and hyperon condensation, superfluidity and quark matter can occur in cores of neutron stars. Specifically, the nuclear to quark matter phase transition and its mixed phases with intriguing structures is treated. Rotating neutron stars with and without phase transitions are discussed and compared to observed masses, radii and glitches. The observations of possible heavy $\sim 2M_{\odot}$ neutron stars in X-ray binaries and QPO's require relatively stiff equation of states and restricts strong phase transitions to occur at very high nuclear densities only.

arXiv:astro-ph/9910200v1 12 Oct 1999

1 INTRODUCTION AND HISTORY OF NEUTRON STARS

It is a great pleasure to participate in the 6'th Colloque Cosmologie at the Observatoire de Paris and stand on the same historic spot, where my fellow countryman Ole Rømer more than two centuries ago first calculated the speed of light¹. I shall therefore start with a brief history of neutron stars and subsequently discuss some very important and recent developments in this field at the turn of this millenium. The most important discoveries concerning neutron stars are briefly listed in Table I. Most are well known except perhaps for the most recent ones, which will be discussed in more detail below.

Table 1
Chronological list of important developments related to neutron stars

Year	“Observers”	Discovery
1054	Chinese	record the Crab Supernova
1572	Tycho Brahe	observes a Supernova
1604	Kepler	observes a Supernova
1932	Chadwick	discovers the neutron
1932	Landau	suggests the existence of neutron stars
1934	Baade & Zwicky	connects supernovae to gravitational collapse of stars to neutron stars
1935	Oppenheimer & Volkoff	calculate neutron star structures with simple EoS
1967	Bell & Hewish	discover first pulsar
1969		pulsars in Crab and Vela Supernova remnants
1973	Hulse & Taylor	discover first binary pulsar
1987	Neutrino detectors	collects 19 neutrinos from SN-1987A
1995	Nijmegen data base	compilation of $\gtrsim 5000$ NN cross sections leads to “modern” NN potentials and EoS
1996	RXTE	discover kHz oscillations (QPO) in X-ray binaries
1997	BeppoSAX	Gamma Ray Burst with afterglow at $z \gtrsim 1$

¹ Actually, he measured and (over-)estimated the light time from the sun, $\sim 12min$, but did not bother to calculate the speed of light because the very distance to the sun was not well known at that time.

2 HEAVY NEUTRON STARS IN X-RAY BINARIES

The best determined neutron star masses are found in binary pulsars and all lie in the range $1.35 \pm 0.04 M_{\odot}$ (see Thorsett and Chakrabarty 1999). These masses have been accurately determined from variations in their radio pulses due to doppler shifts as well periastron advances of their close elliptic orbits that are strongly affected by general relativistic effects. One exception is the nonrelativistic pulsar PSR J1012+5307 of mass² $M = (2.1 \pm 0.8) M_{\odot}$ (van Paradijs 1998).

Several X-ray binary masses have been measured of which the heaviest are Vela X-1 with $M = (1.9 \pm 0.2) M_{\odot}$ (Barziv et al., 1999) and Cygnus X-2 with $M = (1.8 \pm 0.4) M_{\odot}$ (Orosz & Kuulkers 1999). Their Kepler orbits are determined by measuring doppler shift of both the X-ray binary and its companion. To complete the mass determination one needs the orbital inclination which is determined by eclipse durations, optical light curves, or polarization variations (see, e.g., van Paradijs).

The recent discovery of high-frequency brightness oscillations in low-mass X-ray binaries provides a promising new method for determining masses and radii of neutron stars (see Miller, Lamb, & Psaltis 1998). The kilohertz quasi-periodic oscillations (QPO) occur in pairs and are most likely the orbital frequencies

$$\nu_{QPO} = (1/2\pi)\sqrt{GM/R_{orb}^3}, \quad (1)$$

of accreting matter in Keplerian orbits around neutron stars of mass M and its beat frequency with the neutron star spin, $\nu_{QPO} - \nu_s$. According to Zhang, Strohmayer, & Swank 1997, Kaaret, Ford, & Chen (1997) the accretion can for a few QPO's be tracked to its innermost stable orbit,

$$R_{ms} = 6GM/c^2. \quad (2)$$

For slowly rotating stars the resulting mass is from Eqs. (1,2)

$$M \simeq 2.2 M_{\odot} \frac{\text{kHz}}{\nu_{QPO}}. \quad (3)$$

For example, the maximum frequency of 1060 Hz upper QPO observed in 4U 1820-30 gives $M \simeq 2.25 M_{\odot}$ after correcting for the $\nu_s \simeq 275$ Hz neutron star rotation frequency. If the maximum QPO frequencies of 4U 1608-52 ($\nu_{QPO} = 1125$ Hz) and 4U 1636-536 ($\nu_{QPO} = 1228$ Hz) also correspond to innermost stable orbits the corresponding masses are $2.1 M_{\odot}$ and $1.9 M_{\odot}$. Evi-

² The uncertainties are all 95% conf. limits or $\sim 2\sigma$

dence for the innermost stable orbit has only been found for 4U 1820-30, where ν_{QPO} display a distinct saturation with accretion rate indicating that orbital frequency cannot exceed that of the innermost stable orbit. More observations like that are needed before a firm conclusion can be made.

Such large neutron star masses of order $\sim 2M_{\odot}$ severely restrict the equation of state (EoS) for dense matter as addressed in the following.

3 MODERN NUCLEAR EQUATION OF STATES

Recent models for the nucleon-nucleon (NN) interaction, based on the compilation of more than 5000 NN cross sections in the Nijmegen data bank, have reduced the uncertainty in NN potentials. Including many-body effects, three-body forces, relativistic effects, etc., the nuclear EoS have been constructed with reduced uncertainty allowing for more reliable calculations of neutron star properties, see Akmal, Pandharipande, & Ravenhall (1998) and Engvik et al. (1997). Likewise, recent realistic effective interactions for nuclear matter obeying causality at high densities, constrain the EoS severely and thus also the maximum masses of neutron stars, see Akmal, Pandharipande, & Ravenhall (1998) and Kalogera & Baym (1996). We have in [14] elaborated on these analyses by incorporating causality smoothly in the EoS for nuclear matter allowing for first and second order phase transitions to, e.g., quark matter.

For the discussion of the gross properties of neutron stars we will use the optimal EoS of Akmal, Pandharipande, & Ravenhall (1998) (specifically the Argonne $V18+\delta v+UIX^*$ model- hereafter APR98), which is based on the most recent models for the nucleon-nucleon interaction, see Engvik et al. (1997) for a discussion of these models, and with the inclusion of a parametrized three-body force and relativistic boost corrections. The EoS for nuclear matter is thus known to some accuracy for densities up to a few times nuclear saturation density $n_0 = 0.16 \text{ fm}^{-3}$. We parametrize the APR98 EoS by a simple form for the compressional and symmetry energies that gives a good fit around nuclear saturation densities and smoothly incorporates causality at high densities such that the sound speed approaches the speed of light. This requires that the compressional part of the energy per nucleon is quadratic in nuclear density with a minimum at saturation but linear at high densities

$$\begin{aligned} \mathcal{E} &= E_{comp}(n) + S(n)(1 - 2x)^2 \\ &= \mathcal{E}_0 u \frac{u - 2 - s}{1 + su} + S_0 u^\gamma (1 - 2x)^2. \end{aligned} \quad (4)$$

Here, $n = n_p + n_n$ is the total baryon density, $x = n_p/n$ the proton fraction and $u = n/n_0$ is the ratio of the baryon density to nuclear saturation density.

The compressional term is in Eq. (4) parametrized by a simple form which reproduces the saturation density and the binding energy per nucleon $\mathcal{E}_0 = 15.8\text{MeV}$ at n_0 of APR98. The “softness” parameter $s \simeq 0.2$, which gave the best fit to the data of APR98 (see Heiselberg & Hjorth-Jensen 1999) is determined by fitting the energy per nucleon of APR98 up to densities of $n \sim 4n_0$. For the symmetry energy term we obtain $S_0 = 32\text{ MeV}$ and $\gamma = 0.6$ for the best fit. The proton fraction is given by β -equilibrium at a given density.

The one unknown parameter s expresses the uncertainty in the EoS at high density and we shall vary this parameter within the allowed limits in the following with and without phase transitions to calculate mass, radius and density relations for neutron stars. The “softness” parameter s is related to the incompressibility of nuclear matter as $K_0 = 18\mathcal{E}_0/(1 + s) \simeq 200\text{MeV}$. It agrees with the poorly known experimental value (Blaizot, Berger, Decharge, & Girod 1995), $K_0 \simeq 180 - 250\text{MeV}$ which does not restrict it very well. From $(v_s/c)^2 = \partial P/\partial(n\mathcal{E})$, where P is the pressure, and the EoS of Eq. (4), the causality condition $c_s \leq c$ requires

$$s \gtrsim \sqrt{\frac{\mathcal{E}_0}{m_n}} \simeq 0.13, \quad (5)$$

where m_n is the mass of the nucleon. With this condition we have a causal EoS that reproduces the data of APR98 at densities up to $0.6 \sim 0.7\text{ fm}^{-3}$. In contrast, the EoS of APR98 becomes superluminal at $n \approx 1.1\text{ fm}^{-3}$. For larger s values the EoS is softer which eventually leads to smaller maximum masses of neutron stars. The observed $M \simeq 1.4M_\odot$ in binary pulsars restricts s to be less than $0.4 - 0.5$ depending on rotation as shown in calculations of neutron stars below.

In Fig. 1 we plot the sound speed $(v_s/c)^2$ for various values of s and that resulting from the microscopic calculation of APR98 for β -stable pn -matter. The form of Eq. (4), with the inclusion of the parameter s , provides a smooth extrapolation from small to large densities such that the sound speed v_s approaches the speed of light. For $s = 0.0$ ($s = 0.1$) the EoS becomes superluminal at densities of the order of 1 (6) fm^{-3} .

The sound speed of Kalogera & Baym (1996) is also plotted in Fig. 1. It jumps discontinuously to the speed of light at a chosen density. With this prescription they were able to obtain an optimum upper bound for neutron star masses and obey causality. This prescription was also employed by APR98, see Rhoades & Ruffini (1974) for further details. The EoS is thus discontinuously stiffened by taking $v_s = c$ at densities above a certain value n_c which, however, is lower than $n_s = 5n_0$ where their nuclear EoS becomes superluminal. This approach stiffens the nuclear EoS for densities $n_c < n < n_s$ but softens it at higher densities. Their resulting maximum masses lie in the range $2.2M_\odot \lesssim M \lesssim 2.9M_\odot$.

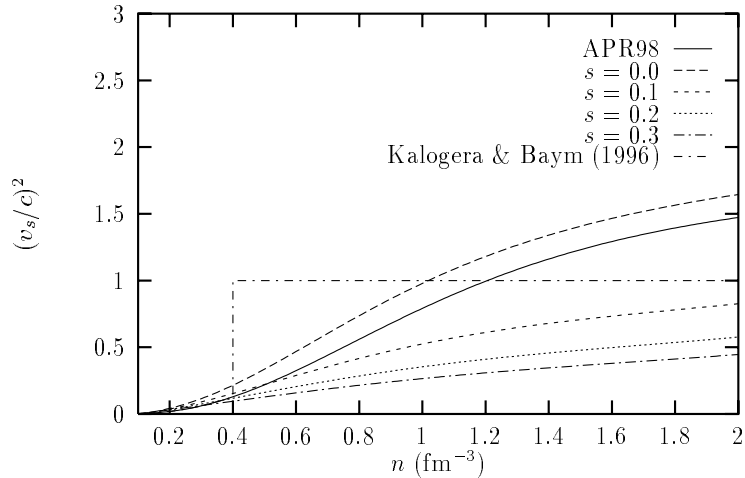


Fig. 1. $(v_s/c)^2$ for β -stable pn -matter for $s = 0, 0.1, 0.2, 0.3$, the results of APR98, and for the patched EoS of Kalogera & Baym (1996) which shows a discontinuous $(v_s/c)^2$.

Our approach however, incorporates causality by reducing the sound speed smoothly towards the speed of light at high densities. Therefore our approach will not yield an absolute upper bound on the maximum mass of a neutron star but gives reasonable estimates based on modern EoS around nuclear matter densities, causality constraints at high densities and a smooth extrapolation between these two limits (see Fig. 1).

At very high densities particles are expected to be relativistic and the sound speed should be smaller than the speed of light, $v_s^2 \simeq c^2/3$. Consequently, the EoS should be even softer at high densities and the maximum masses we obtain with the EoS of (4) are likely to be too high estimates.

4 PHASE TRANSITIONS

The physical state of matter in the interiors of neutron stars at densities above a few times normal nuclear matter densities is essentially unknown and many first and second order phase transitions have been speculated upon. We will specifically study the hadron to quark matter transition at high densities, but note that other transitions as, e.g., kaon and/or pion condensation or the presence of other baryons like hyperons also soften the EoS and thus further aggravate the resulting reduction in maximum masses. Hyperons appear at densities typically of the order $2n_0$ and result in a considerable softening of the EoS, see e.g., Balberg, Lichenstadt, & Cook (1998). Typically, most equations of state with hyperons yield masses around $1.4 - 1.6M_\odot$. Here however, in order to focus on the role played by phase transitions in neutron star matter, we will assume that a phase transition from nucleonic to quark matter takes place at a certain density. Since we do not have a fully reliable theory for the quark matter phase, we will for simplicity employ the bag model in our actual studies of quark phases and neutron star properties. In the bag model the quarks are assumed to be confined to a finite region of space, the so-called 'bag', by a vacuum pressure B . Adding the Fermi pressure and interactions computed to order $\alpha_s = g^2/4\pi$, where g is the QCD coupling constant, the total pressure for 3 massless quarks of flavor $f = u, d, s$, is (see Kapusta (1988)),

$$P = \frac{3\mu_f^4}{4\pi^2} \left(1 - \frac{2}{\pi}\alpha_s\right) - B + P_e + P_\mu, \quad (6)$$

where $P_{e,\mu}$ are the electron and muon pressure, e.g., $P_e = \mu_e^4/12\pi^2$. A Fermi gas of quarks of flavor i has density $n_i = k_{Fi}^3/\pi^2$, due to the three color states. A finite strange quark mass have minor effect on the EoS since quark chemical potentials $\mu_q \gtrsim m_N/3$ typically are much larger. The value of the bag constant B is poorly known, and we present results using two representative values, $B = 150 \text{ MeVfm}^{-3}$ and $B = 200 \text{ MeVfm}^{-3}$. We take $\alpha_s = 0.4$. However, similar results can be obtained with smaller α_s and larger B (Madsen 1998).

The quark and nuclear matter mixed phase described in Glendenning (1992) has continuous pressures and densities due to the general Gibbs criteria for two-component systems. There are no first order phase transitions but at most two second order phase transitions. Namely, at a lower density, where quark matter first appears in nuclear matter, and at a very high density (if gravita-

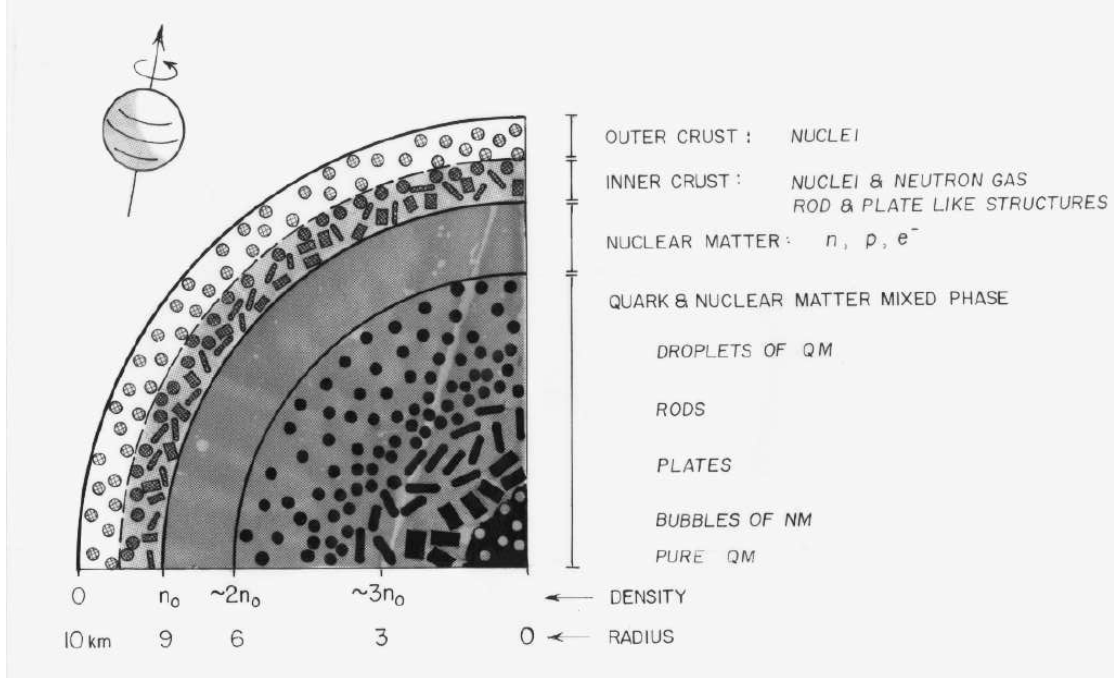


Fig. 2. The quark and nuclear matter structure in a quarter of a typical $1.4M_{\odot}$ solar mass neutron star. The typical sizes of structures are a few Fermi's but have been scaled up by about 16 orders of magnitudes to be seen.

tionally stable), where all nucleons are finally dissolved into quark matter. This mixed phase does, however, not include local surface and Coulomb energies of the quark and nuclear matter structures. If the interface tension between quark and nuclear matter is too large, the mixed phase is not favored energetically due to surface and Coulomb energies associated with forming these structures (Heiselberg, Pethick, & Staubo 1993). The neutron star will then have a core of pure quark matter with a mantle of nuclear matter surrounding it and the two phases are coexisting by a first order phase transition or Maxwell construction. For a small or moderate interface tension the quarks are confined in droplet, rod- and plate-like structures as found in the inner crust of neutron stars (Lorenz, Ravenhall, & Pethick 1993).

5 MASSES AND RADII OF NEUTRON STARS

In order to obtain the mass and radius of a neutron star, we have solved the Tolman-Oppenheimer-Volkov equation with and without rotational corrections following the approach of Hartle (1967). The equations of state employed are given by the pn -matter EoS with $s = 0.13, 0.2, 0.3, 0.4$ with nucleonic de-

degrees of freedom only. In addition we have selected two representative values for the bag-model parameter B , namely 150 and 200 MeVfm $^{-3}$ for our discussion on eventual phase transitions. The quark phase is linked with our pn -matter EoS from Eq. (4) with $s = 0.2$ through either a mixed phase construction or a Maxwell construction, see Heiselberg and Hjorth-Jensen (1999) for further details. For $B = 150$ MeVfm $^{-3}$, the mixed phase begins at 0.51 fm $^{-3}$ and the pure quark matter phase begins at 1.89 fm $^{-3}$. Finally, for $B = 200$ MeVfm $^{-3}$, the mixed phase starts at 0.72 fm $^{-3}$ while the pure quark phase starts at 2.11 fm $^{-3}$. In case of a Maxwell construction, in order to link the pn and the quark matter EoS, we obtain for $B = 150$ MeVfm $^{-3}$ that the pure pn phase ends at 0.92 fm $^{-3}$ and that the pure quark phase starts at 1.215 fm $^{-3}$, while the corresponding numbers for $B = 200$ MeVfm $^{-3}$ are 1.04 and 1.57 fm $^{-3}$.

None of the equations of state from either the pure pn phase or with a mixed phase or Maxwell construction with quark degrees of freedom, result in stable configurations for densities above $\sim 10n_0$, implying thereby that none of the stars have cores with a pure quark phase. The EoS with pn degrees of freedom have masses $M \lesssim 2.2M_\odot$ when rotational corrections are accounted for. With the inclusion of the mixed phase, the total mass is reduced since the EoS is softer. However, there is the possibility of making very heavy quark stars for very small bag constants. For pure quark stars there is only one energy scale namely B which provides a homology transformation (Madsen 1998) and the maximum mass is $M_{max} = 2.0M_\odot(58\text{MeVfm}^{-3}/B)^{1/2}$ (for $\alpha_s = 0$). However, for $B \gtrsim 58\text{MeVfm}^{-3}$ a nuclear matter mantle has to be added and for $B \lesssim 58\text{MeVfm}^{-3}$ quark matter has lower energy per baryon than ^{56}Fe and is thus the ground state of strongly interacting matter. Unless the latter is the case, we can thus exclude the existence of $2.2 - 2.3M_\odot$ quark stars.

In Fig. 5 we show the mass-radius relations for the various equations of state. The shaded area represents the allowed masses and radii for $\nu_{QPO} = 1060$ Hz of 4U 1820-30. Generally,

$$2GM < R < \left(\frac{GM}{4\pi^2\nu_{QPO}^2} \right)^{1/3}, \quad (7)$$

where the lower limit insures that the star is not a black hole, and the upper limit that the accreting matter orbits outside the star, $R < R_{orb}$. Furthermore, for the matter to be outside the innermost stable orbit, $R > R_{ms} = 6GM$, requires that

$$M \lesssim \frac{1 + 0.75j}{12\sqrt{6}\pi G\nu_{QPO}} \simeq 2.2M_\odot(1 + 0.75j) \frac{\text{kHz}}{\nu_{QPO}}, \quad (8)$$

where $j = 2\pi c\nu_s I/M^2$ is a dimensionless measure of the angular momentum of the star with moment of inertia I . The upper limit in Eq. (8) is the mass

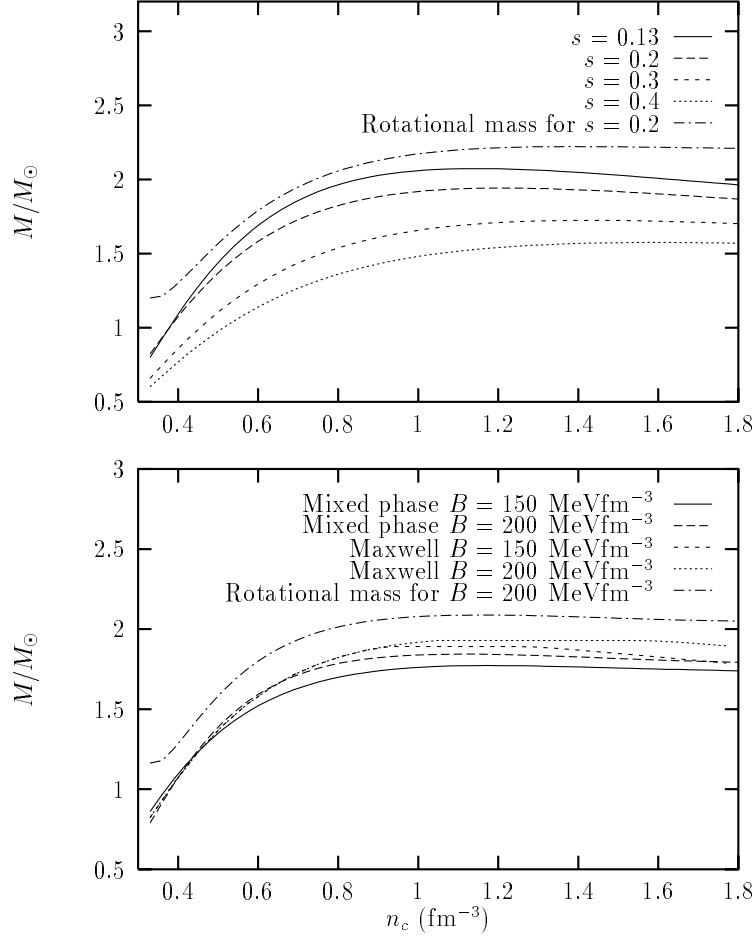


Fig. 3. Total mass M as function of central density n_c for various values of s (upper panel) and the bag parameter B (lower panel) for both a mixed phase and a Maxwell constructed EoS with $s = 0.2$ in Eq. 4). In addition we include also the rotational corrections for the pure pn -case with $s = 0.2$ and the mixed phase construction for $B = 200 \text{ MeVfm}^{-3}$. For the Maxwell construction which exhibits a first order phase transition, in the density regions where the two phases coexist, the pressure is constant, a fact reflected in the constant value of the neutron star mass. All results are for β -stable matter. Note also that for the upper panel, the EoS for $s = 0.3$ and $s = 0.4$ start to differ from those with $s = 0.13, 0.2$ at densities below 0.2 fm^{-3} .

when ν_{QPO} corresponds to the innermost stable orbit. According to Zhang, Smale, Strohmayer & Swank (1998) this is the case for 4U 1820-30 since ν_{QPO} saturates at ~ 1060 Hz with increasing count rate. The corresponding neutron star mass is $M \sim 2.2 - 2.3M_{\odot}$ which leads to several interesting conclusions as seen in Fig. 5. Firstly, the stiffest EoS allowed by causality ($s \simeq 0.13 - 0.2$) is needed. Secondly, rotation must be included which increase the maximum mass and corresponding radii by 10-15% for $\nu_s \sim 300$ Hz. Thirdly, a phase transition to quark matter below densities of order $\sim 5n_0$ can be excluded, corresponding to a restriction on the bag constant $B \gtrsim 200 \text{ MeVfm}^{-3}$.

These maximum masses are smaller than those of APR98 and Kalogera & Baym (1996) who, as discussed above, obtain upper bounds on the mass of neutron stars by discontinuously setting the sound speed to equal the speed of light above a certain density, n_c . By varying the density $n_c = 2 \rightarrow 5n_0$ the maximum mass drops from $2.9 \rightarrow 2.2M_{\odot}$. In our case, incorporating causality smoothly by introducing the parameter s in Eq. (4), the EoS is softened at higher densities in order to obey causality, and yields a maximum mass which instead is slightly lower than the $2.2M_{\odot}$ derived in APR98 for nonrotating stars.

If the QPOs are not from the innermost stable orbits and one finds that even accreting neutron stars have small masses, say like the binary pulsars, $M \lesssim 1.4M_{\odot}$, this may indicate that heavier neutron stars are not stable. Therefore, the EoS is soft at high densities $s \gtrsim 0.4$ or that a phase transition occurs at a few times nuclear matter densities. For the nuclear to quark matter transition this would require $B < 80 \text{ MeVfm}^{-3}$ for $s = 0.2$. For such small bag parameters there is an appreciable quark and nuclear matter mixed phase in the neutron star interior but even in these extreme cases a pure quark matter core is not obtained for stable neutron star configurations.

6 GLITCHES

Younger pulsars rotate and slow down rapidly. Some display sudden speed ups referred to as glitches. We shall first discuss such standard glitches and subsequently continue to giant glitches and other characteristic glitch behavior for spin frequencies close to the critical ones, where first order phase transitions occur at densities present right at the core of neutron stars.

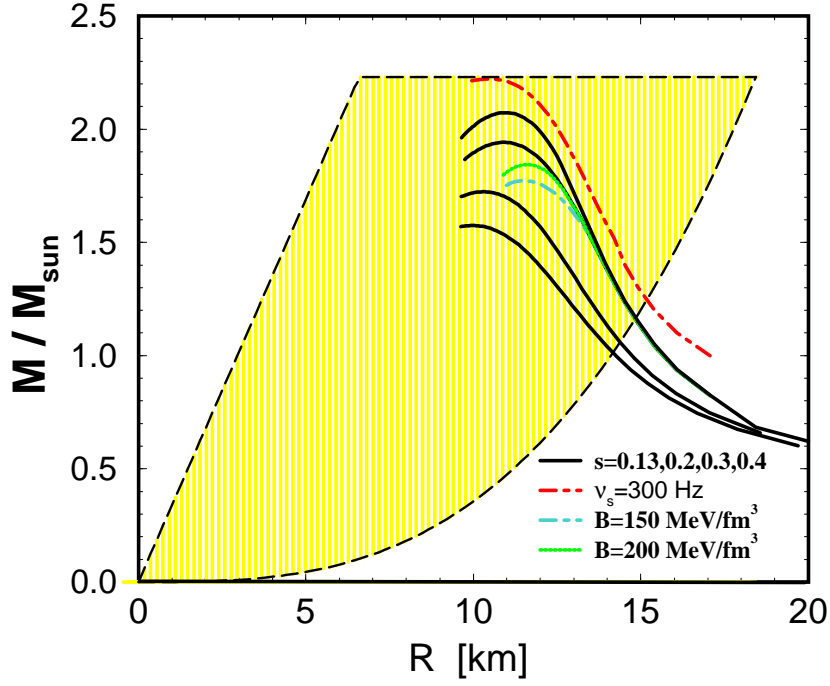


Fig. 4. Neutron star masses vs. radius for the EoS of Eq. (1) with softness $s=0.13,0.2,0.3,0.4$, with increasing values of s from top to bottom for the full curves. Phase transitions decrease the maximum mass whereas rotation increases it. The shaded area represents the neutron star radii and masses allowed (see text and Eqs. 1-3) for orbital QPO frequencies 1060 Hz of 4U 1820-30.

6.1 Core quakes and glitches

The glitches observed in the Crab, Vela, and a few other pulsars are probably due to quakes occurring in solid structures such as the crust, superfluid vortices or possibly the quark matter lattice in the core [16]. As the rotating neutron star gradually slows down and becomes less deformed, the rigid component is strained and eventually cracks/quakes and changes its structure towards being more spherical.

The moment of inertia of the rigid component, I_c , decreases abruptly and its rotation and pulsar frequency increases due to angular momentum conservation resulting in a glitch. The observed glitches are very small $\Delta\Omega/\Omega \sim 10^{-8}$. The two components slowly relaxate to a common rotational frequency on a time scale of days (healing time) due to superfluidity of the other component (the neutron liquid). The *healing parameter* $Q = I_c/I_{tot}$ measured in glitches reveals that for the Vela and Crab pulsar about $\sim 3\%$ and $\sim 96\%$ of the moment of inertia is in the rigid component respectively.

If the crust were the only rigid component the Vela neutron star should be almost all crust. This would require that the Vela is a very light neutron star - much smaller than the observed ones which all are compatible with $\sim 1.4M_\odot$. If we by the lattice component include not only the solid crust but also the protons in nuclear matter (NM) (which is locked to the crust due to magnetic fields), superfluid vortices pinned to the crust [27] and the solid QM mixed phase

$$I_c = I_{crust} + I_p + I_{sv} + I_{QM}, \quad (9)$$

we can better explain the large I_c for the Crab. The moment of inertia of the mixed phase is sensitive to the EoS's used. For example, for a quadratic NM EoS [16] decreasing the Bag constant from 110 to 95 MeVfm⁻³ increases I_c/I_{total} from $\sim 20\%$ to $\sim 70\%$ for a $1.4M_\odot$ neutron star - not including possible vortex pinning. The structures in the mixed phase would exhibit anisotropic elastic properties, being rigid to some shear strains but not others in much the same way as liquid crystals. Therefore the whole mixed phase might not be rigid.

The energy released in glitches every few years are too large to be stored in the crust only. The recurrence time for large quakes, t_c , is inversely proportional to the strain energy [27], which again is proportional to the lattice density and the Coulomb energy

$$t_c^{-1} \propto \frac{1}{a^3} \frac{Z^2 e^2}{a}. \quad (10)$$

Since the lattice distance a is smaller for the quark matter droplets and their charge larger than for atoms in the crust, the recurrence time is shorter in better agreement with measurements of large glitches.

Detecting core and crust quakes separately or other signs of three components in glitches, indicating the existence of a crust, superfluid neutrons and a solid core, would support the idea of the mixed quark and nuclear matter mixed phase. However, magnetic field attenuation is expected to be small in neutron stars and therefore magnetic fields penetrate through the core. Thus the crust and core lattices as well as the proton liquid should be strongly coupled and glitch simultaneously.

6.2 Backbending and giant glitches

In [11] the moment of inertia is found to “backbend” as function of angular velocity. The moment of inertia of some deformed nuclei [24,17] may also backbend when the coriolis force exceeds the pairing force breaking the pair-

ing whereby the nucleus reverts from partial superfluidity to a rigid rotor. However, in the limit of large nuclear mass number such backbending would disappear. Instead pairing may lead to superfluidity in bulk [27]. A backbending phenomenon in neutron stars, that appears to be similar to backbending in nuclei, can occur in neutron stars although the physics behind is entirely different. If we soften the EoS significantly at a density near the central density of the neutron star, a non-rotating neutron star can have most of its core at high densities where the soft EoS determines the profile. A rapidly rotating star may instead have lower central densities only probing the hard part of the EoS. Thus the star may at a certain angular velocity revert from the dense phase to a more dilute one and at the same time change its structure and moment of inertia discontinuously. Such a drastic change in moment of inertia at some angular velocity will cause a giant glitch as found in [11].

The phenomenon of neutron star backbending is related to the double maximum mass for a neutron and quark star respectively as discussed in Ref. [14]. Both phenomena occur when the “softening” or density discontinuity exceeds

$$\varepsilon_2 \gtrsim \frac{3}{2} \varepsilon_1 \quad \Rightarrow \quad \text{Two maximum masses and Giant glitch when } \omega \simeq \omega_0. \quad (11)$$

Similarly, there is also a discontinuity in the moment of inertia when $\rho_2/\rho_1 \gtrsim 3/2$. The neutron star may continue to slow down in its unstable structure, i.e. “super-rotate”, before reverting to its stable configuration with a dense core. As for the instabilities of Eq. (11) this condition changes slightly for a more general EoS and when general relativity is included. Neutron stars with a mixed phase do not have a first order phase transition but may soften their EoS sufficiently that a similar phenomenon occurs [11]. We emphasize, however, that the discontinuous jump in moment of inertia is due to the drastic and sudden softening of the EoS near the central density of neutron stars. It is not important whether it is a phase transition or another phenomenon that causes the softening.

6.3 Phase transitions in rotating neutron stars

During the last years, and as discussed in the previous sections, interesting phase transitions in nuclear matter to quark matter, mixed phases of quark and nuclear matter [10,16], kaon [20] or pion condensates [1], neutron and proton superfluidity [8], hyperonic matter [33,32,21] crystalline nuclear matter, magnetized matter, etc., have been considered. Here we consider the interesting phenomenon of how the star and in particular its moment of inertia behaves near the critical angular velocity, Ω_0 , where the core pressure just exceeds that needed to make a phase transition.

As described in detail in [14] the general relativistic equations for slowly rotating stars can be solved even with first order phase transitions. The resulting moment of inertia have the characteristic behavior for $\Omega \lesssim \Omega_0$ (see also Fig. (5))

$$I = I_0 \left(1 + \frac{1}{2} c_1 \frac{\Omega^2}{\Omega_0^2} - \frac{2}{3} c_2 \left(1 - \frac{\Omega^2}{\Omega_0^2} \right)^{3/2} + \dots \right). \quad (12)$$

For the two incompressible fluids with momentum of inertia, the small expansion parameters are $c_1 = \omega_0^2$ and $c_2 = (5/2)\omega_0^3(\varepsilon_2/\varepsilon_1 - 1)/(3 - 2\varepsilon_2/\varepsilon_1 - \omega_0^2)^{3/2}$; for $\Omega > \Omega_0$ the c_2 term is absent. For a Bethe-Johnson polytropic EoS we find from Fig. (5) that $c_2 \simeq 0.07 \simeq 2.2\omega_0^3$. Generally, we find that the coefficient c_2 is proportional to the density difference between the two coexisting phases and to the critical angular velocity to the third power, $c_2 \sim (\varepsilon_2/\varepsilon_1 - 1)\omega_0^3$. The scaled critical angular velocity ω_0 can at most reach unity for submillisecond pulsars.

To make contact with observation we consider the temporal behavior of angular velocities of pulsars. The pulsars slow down at a rate given by the loss of rotational energy which we shall assume is proportional to the rotational angular velocity to some power (for dipole radiation $n = 3$)

$$\frac{d}{dt} \left(\frac{1}{2} I \Omega^2 \right) = -C \Omega^{n+1}. \quad (13)$$

With the moment of inertia given by Eq. (12) the angular velocity will then decrease with time as

$$\begin{aligned} \frac{\dot{\Omega}}{\Omega} &= -\frac{C \Omega^{n-1}}{I_0} \left(1 - c_1 \frac{\Omega^2}{\Omega_0^2} - c_2 \sqrt{1 - \frac{\Omega^2}{\Omega_0^2}} \right) \\ &\simeq -\frac{1}{(n-1)t} \left(1 - c_2 \sqrt{1 - \left(\frac{t_0}{t} \right)^{2/(n-1)} + \dots} \right), \end{aligned} \quad (14)$$

for $t \geq t_0$. Here, the time after formation of the pulsar is, using Eq. (13), related to the angular velocity as $t \simeq t_0(\Omega_0/\Omega)^{n-1}$ and $t_0 = I_0/((n-1)C\Omega_0^{n-1})$ for $n > 1$, is the critical time where a phase transition occurs in the center. For earlier times $t \leq t_0$ there is no dense core and Eq. (14) applies when setting $c_2 = 0$. The critical angular velocity is $\Omega_0 = \omega_0 \sqrt{2\pi\varepsilon_1} \simeq 6kH z$ for the Bethe-Johnson EoS [4], i.e. comparable to a millisecond binary pulsar. Applying these numbers to, for example, the Crab pulsar we find that it would have been spinning with critical angular velocity approximately a decade after the Crab supernova explosion, i.e. $t_0 \sim 10$ years for the Crab. Generally, $t_0 \propto \Omega_0^{1-n}$ and the timescale for the transients in $\dot{\Omega}$ as given by Eq. (13) may be months or centuries. In any case it would not require continuous monitoring which would help a dedicated observational program.

The braking index depends on the second derivative $I'' = dI/d^2\Omega$ of the moment of inertia and thus diverges (see Fig. (1)) as Ω approaches Ω_0 from below

$$n(\Omega) \equiv \frac{\ddot{\Omega}\Omega}{\dot{\Omega}^2} \simeq n - 2c_1 \frac{\Omega^2}{\Omega_0^2} + c_2 \frac{\Omega^4/\Omega_0^4}{\sqrt{1 - \Omega^2/\Omega_0^2}}. \quad (15)$$

For $\Omega \geq \Omega_0$ the term with c_2 is absent. The *observational* braking index $n(\Omega)$ should be distinguished from the *theoretical* exponent n appearing in Eq. (12). Although the results in Eqs. (13) and (14) were derived for the pulsar slow down assumed in Eq. (12) both $\dot{\Omega}$ and $n(\Omega)$ will generally display the $\sqrt{t - t_0}$ behavior for $t \geq t_0$ as long as the rotational energy loss is a smooth function of Ω . The singular behavior will, however, be smeared on the pulsar glitch “healing” time which in the case of the Crab pulsar is of order weeks only.

We now discuss possible phase transitions in interiors of neutron stars. The quark and nuclear matter mixed phase described in [10] has continuous pressures and densities. There are no first order phase transitions but at most two second order phase transitions. Namely, at a lower density, where quark matter first appears in nuclear matter, and at a very high density (if gravitationally stable), where all nucleons are finally dissolved into quark matter. In second-order phase transitions the pressure is a continuous function of density and we find a continuous braking index. This mixed phase does, however, not include local surface and Coulomb energies of the quark and nuclear matter structures. As shown in [16] there can be an appreciable surface and Coulomb energy associated with forming these structures and if the interface tension between quark and nuclear matter is too large, the mixed phase is not favored energetically. The neutron star will then have a core of pure quark matter with a mantle of nuclear matter surrounding it and the two phases are coexisting by a first order phase transition. For a small or moderate interface tension the quarks are confined in droplet, rod- and plate-like structures as found in the inner crust of neutron stars [22]. Due to the finite Coulomb and surface energies associated with forming these structures, the transitions change from second order to first order at each topological change in structure. If a Kaon condensate appears it may also have such structures [12]. Pion condensates [7], crystalline nuclear matter [1], hyperonic or magnetized matter, etc. may provide other first order phase transitions.

Thus, if a first order phase transitions is present at central densities of neutron stars, it will show up in moments of inertia and consequently also in angular velocities in a characteristic way. For example, the slow down of the angular velocity has a characteristic behavior $\dot{\Omega} \sim c_2 \sqrt{1 - t/t_0}$ and the braking index diverges as $n(\Omega) \sim c_2/\sqrt{1 - \Omega^2/\Omega_0^2}$ (see Eqs. (14) and (15)). The magnitude of the signal generally depends on the density difference between the two phases

and the critical angular velocity $\omega_0 = \Omega_0/\sqrt{2\pi\varepsilon_1}$ such that $c_2 \sim (\varepsilon_2/\varepsilon_1 - 1)\omega_0^3$. The observational consequences depend very much on the critical angular velocity Ω_0 , which depends on the EoS employed, at which density the phase transition occurs and the mass of the neutron star.

We encourage a dedicated search for the characteristic transients discussed above. As the pulsar slows down over a million years, its central densities spans a wide range of order $1n_0$ (see Fig. 5). As we are interested in time scales of years, we must instead study all ~ 1000 pulsars available. By studying the corresponding range of angular velocities for the sample of different star masses, the chance for encountering a critical angular velocity increases. Eventually, one may be able to cover the full range of central densities and find all first order phase transitions up to a certain size determined by the experimental resolution. Since the size of the signal scales with Ω_0^3 the transition may be best observed in rapidly rotating pulsars such as binary pulsars or pulsars recently formed in supernova explosion and which are rapidly slowing down. Carefully monitoring such pulsars may reveal the characteristic behavior of the angular velocity or braking index as described above which is a signal of a first order phase transition in dense matter.

7 SUMMARY

Modern nucleon-nucleon potentials have reduced the uncertainties in the calculated EoS. Using the most recent realistic effective interactions for nuclear matter of APR98 with a smooth extrapolation to high densities including causality, the EoS could be constrained by a “softness” parameter s which parametrizes the unknown stiffness of the EoS at high densities. Maximum masses have subsequently been calculated for rotating neutron stars with and without first and second order phase transitions to, e.g., quark matter at high densities.

The calculated bounds for maximum masses leaves two natural options when compared to the observed neutron star masses:

- **Case I:** *The large masses of the neutron stars in QPO 4U 1820-30 ($M = 2.3M_\odot$), PSR J1012+5307 ($M = 2.1 \pm 0.4M_\odot$), Vela X-1 ($M = 1.9 \pm 0.1M_\odot$), and Cygnus X-2 ($M = 1.8 \pm 0.2M_\odot$), are confirmed and complemented by other neutron stars with masses around $\sim 2M_\odot$.*

As a consequence, the EoS of dense nuclear matter is severely restricted and only the stiffest EoS consistent with causality are allowed, i.e., softness parameter $0.13 \leq s \lesssim 0.2$. Furthermore, any significant phase transition at densities below $< 5n_0$ can be excluded.

That the radio binary pulsars all have masses around $1.4M_\odot$ is then proba-

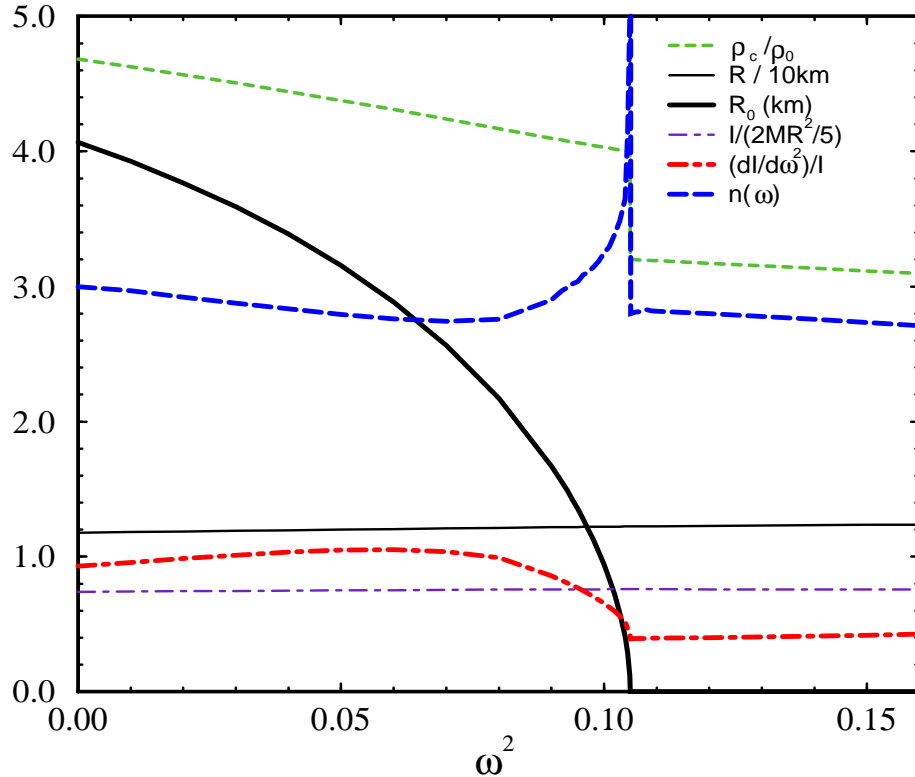


Fig. 5. Central density (in units of ε_0), radii of the neutron star R and its dense core R_0 , moment of inertia, its derivative $I'/I = dI/d\omega^2/I$ and the braking index are shown as function of the scaled angular velocity $\omega^2 = \Omega^2/(2\pi\varepsilon_1)$. The rotating neutron star has mass $1.4M_\odot$ and a Bethe-Johnson like polytropic EoS with a first order phase transition taking place at density $\varepsilon_1 = 3.2\varepsilon_0$ to $\varepsilon_2 = 4\varepsilon_0$.

bly due to the formation mechanism in supernovae where the Chandrasekhar mass for iron cores are $\sim 1.5M_\odot$. Neutron stars in binaries can subsequently acquire larger masses by accretion as X-ray binaries.

- **Case II:** *The heavy neutron stars prove erroneous by more detailed observations and only masses like those of binary pulsars are found.*

If accretion does not produce neutron stars heavier than $\gtrsim 1.4M_\odot$, this indicates that heavier neutron stars simply are not stable which in turn implies a soft EoS, either $s > 0.4$ or a significant phase transition must occur already at a few times nuclear saturation densities.

Surface temperatures can be estimated from spectra and from the measured fluxes and known distances, one can extract the surface area of the emitting spot. This gives unfortunately only a lower limit on the neutron star size, R . If it becomes possible to measure both mass and radii of neutron stars, one

can plot an observational (M, R) curve in Fig. (5), which uniquely determines the EoS for strongly interacting matter at zero temperature.

Pulsar rotation frequencies and glitches are other promising signals that could reveal phase transitions. Besides the standard glitches also giant glitches were mentioned and in particular the characteristic behavior of angular velocities when a first order phase transition occurs right in the center of the star.

It is, unfortunately, impossible to cover all the interesting and recent developments concerning neutron stars in these proceedings so for more details we refer to [14] and Refs. therein.

Acknowledgements: to my collaborators M. Hjorth-Jensen and C.J. Pethick as well as G. Baym, F. Lamb and V. Pandharipande.

References

- [1] Akmal, A., Pandharipande, V. R., & Ravenhall, D. G., 1998, Phys. Rev. C, 58, 1804
- [2] Balberg, S., Lichenstadt, I., & Cook, G. B., 1998, preprint astro-ph/9810361
- [3] Barziv et al., 1999, in preparation; earlier analyses (van Kerkwijk, M. H., van Paradijs, J., & Zuiderwijk, E. J., 1995, A. & A., 303, 497) have larger uncertainties.
- [4] H.A. Bethe and M.B. Johnson, Nucl. Phys. A 230 (1974) 1.
- [5] Blaizot, J. P., Berger, J. F., Decharge, J., & Girod, M., 1995, nucl. phys. A, 591, 435
- [6] Baym, G. A., & Chin, S. A., 1976, nucl. phys. A, 262, 527.
- [7] G. Baym and C.J. Pethick, Ann. Rev. Nucl. Sci. 25 (1975) 27; Ann. Rev. Astron. Astrophys. 17 (1979) 415.
- [8] Ø. Elgarøy, L. Engvik, M Hjorth-Jensen and E. Osnes, Phys. Rev. Lett. 77 (1996) 1421.
- [9] Engvik, L., Hjorth-Jensen, M., Machleidt, R., Muther, H., & Polls A., 1997, nucl. phys. A, 627, 125
- [10] Glendenning, N.K. , 1992, Phys. Rev. D, 46, 1274
- [11] N.K. Glendenning, S. Pei and F. Weber, Phys. Rev. Lett. 79 (1997) 1603.
- [12] N.K. Glendenning and J. Schaffner, Phys. Rev. Lett. 81 (1998) 4564.
- [13] Hartle, J. B., 1967, Ap.J., 150, 1005

- [14] Heiselberg, H., & Hjorth-Jensen, M., 1998, *Phys. Rev. Lett.*, 80, 5485; and 1999, *Phys. Rep.*, in press
- [15] Heiselberg, H., & Hjorth-Jensen, M., 1998, *Ap.J.*, in press
- [16] Heiselberg, H., Pethick, C. J., & Staubo, E. F., 1993, *Phys. Rev. Lett.*, 70, 1355
- [17] A. Johnson, H. Ryde and S.A. Hjorth, *Nucl. Phys. A* 179 (1972) 753.
- [18] Kaaret, P., Ford, E. C., & Chen, K., 1997, *Ap.J.Lett.*, 480, L27
- [19] Kalogera, V., & Baym, G., 1996, *Ap.J.Lett.*, 470, L61
- [20] D.B. Kaplan and A.E. Nelson, *Phys. Lett. B* 291 (1986) 57.
- [21] R. Knorren, M. Prakash and P.J. Ellis, *Phys. Rev. C* 52 (1995) 3470.
- [22] Lorenz, C. P., Ravenhall, D. G., & Pethick, C. J., 1993, *Phys. Rev. Lett.*, 70, 379
- [23] J. Madsen, preprint astro-ph/9809032 and references therein.
- [24] B.R. Mottelson and J.G. Valatin, *Phys. Rev. Lett.* 5 (1960) 511.
- [25] Miller, M. C., Lamb, F. K., & Psaltis, P., 1998 *Ap.J.*, 508, 791.
- [26] Orosz, J. A., & Kuulkers, E., 1999, *Mon. Not. R. Astron. Soc.*, in press
- [27] D. Pines, in: *Neutrons stars: theory and observation of the Neutron Stars*, eds. J. Alpar and D. Pines, (Kluwer, Dordrecht, 1991) p. 57, and references therein; P.W. Anderson and N. Itoh, *Nature* 256 (1975) 25.
- [28] Psaltis D. et al., astro-ph/9903105, *Ap.J.*, in press
- [29] van Paradijs, J., 1998, astro-ph/9802177 and in: *The Many Faces of Neutron Stars*, ed. R. Buccheri, J. van Paradijs & M. A. Alpar, (Dordrecht: Kluwer), in press
- [30] Rhoades, C. E., Jr., & Ruffini, R, 1974, *Phys. Rev. Lett.*,32, 324
- [31] Schaab, C., Weigel, M.K., 1999, *Mon. Not. R. Astron. Soc.*, in press
- [32] J. Schaffner and I. Mishustin, *Phys. Rev. C* 53 (1996) 1416.
- [33] H.-J. Schulze, M. Baldo, U. Lombardo, J. Cugnon and A. Lejeune, *Phys. Rev. C* 57 (1998) 704; M. Baldo, G.F. Burgio and H.-J. Schulze, *Phys. Rev. C* 58 (1998) 3688.
- [34] Stella, L., Vietri M., 1998, *ApJ*, 492, L59
- [35] Thorsett, S. E., & Chakrabarty, D., 1999, *Ap.J.*, 512, 288
- [36] Zhang, W., Strohmayer, T. E., & Swank, J. H., 1997, *Ap.J.Lett.*, 482, L167
- [37] Zhang, W., Smale, A. P., Strohmayer, T. E., & Swank, J. H., 1998, *Ap.J.Lett.*, 500, L171